2656 *Inorg. Chem.* **2010**, *49*, 2656–2666
DOI: 10.1021/ic901651d

Inorganic Chemistry
Article

Structural Variety within Gallium Diphosphonates Affected by the Organic Linker Length

Martin P. Attfield,*,† Zhanhui Yuan,‡ Howard G. Harvey,§ and William Clegg*,‡

†*Centre for Nanoporous Materials, School of Chemistry, The University of Manchester, Oxford Road, Manchester, M13 9PL, U.K.,* ‡*School of Chemistry, Newcastle University, Newcastle upon Tyne, NE1 7RU, U.K., and* §*Davy-Faraday Research Laboratory, The Royal Institution of Great Britain, 21 Albemarle Street, London, W1S 4BS, U.K.*

Received August 18, 2009

Three new gallium diphosphonates: $Ga_3(OH)(O_3PC_3H_6PO_3)_2$ (**1**), $Ga_4(O_3PC_5H_{10}PO_3)_3(C_5H_5N)_2$ (**2**), and $Ga(HO_3PC_{10}H_{20}PO_3)$ (**3**), in which the diphosphonate bridging ligands have 3, 5, and 10 methylene units, respectively, have been synthesized using solvothermal methods and their structures determined using single-crystal laboratory and synchrotron X-ray diffraction data. All three materials contain Ga-centered tetrahedra and octahedra linked together through the $-PO_3$ groups of the diphosphonate ligands to form two-dimensional pillared slab (**1**) and three-dimensional pillared (**2** and **3**) materials. Compound **1** contains bridging hydroxide anions that connect Ga-centered octahedra and tetrahedra, and contains pillared slabs in which one side of the Ga−P−O/OH/CH hybrid layers are connected by the propylenediphosphonate groups only. This slab also contains propylenediphosphonate groups arranged orthogonally to the pillaring direction in the outermost layer of the Ga−P−O/OH/CH hybrid layers. Compound **2** is a framework structure that contains framework pyridine molecules between alternate layers of diphosphonate-pillared Ga−P−O layers and is structurally stable to loss of 1 equiv of pyridine molecules from the structure. Compound **3** is a partially condensed pillared framework structure with one P−O−H bond per diphosphonate group remaining in the resulting material. The structural changes observed as the alkylene chain in the diphosphonate ligand is increased in these compounds is compared to other members of the gallium diphosphonate family synthesized in a similar manner, and other metal diphosphonate series, to gain some general oversight of the structural trends observed in series of metal diphosphonate materials in which the alkylene chain length is varied systematically.

Introduction

Inorganic−organic hybrid materials have become a major theme of materials chemistry over the last 20 years.[1] The attraction of these hybrid materials stems from the benefits introduced by inclusion of both inorganic and organic components into the product. In particular, the incorporation and modification of organic groups within structures allows the possibility of designing materials with specific structural and chemical properties. The former is a particularly desirable attribute in the synthesis of microporous materials whose properties are heavily determined by the internal framework structure of the material.[2] Mono-, di-, tri-, and tetra-phosphonic acids are excellent precursors for the preparation of such hybrid materials and have led to the formation of a wide variety of structures containing zero-,[3,4] one-,[5] two-,[6] and three-dimensional inorganic components.[7,8] The resulting metal phosphonate materials have displayed potential for application in areas such as sorption,[9] ion exchange,[10] sensing,[11,12] charge storage,[13] and catalysis.[14,15]

*To whom correspondence should be addressed. E-mail: m.attfield@manchester.ac.uk. Phone: 00-44-161-306-4467. Fax: 00-44-161-275-4598.

(1) (a) Rao, C. N. R.; Cheetham, A. K.; Thirumurugan, A. *J. Phys.: Condens. Matter* **2008**, *20*, 083202. (b) Rowsell, J. L. C.; Yaghi, O. M. *Microporous Mesoporous Mater.* **2004**, *73*, 3. (c) Cariati, E.; Pizzotti, M.; Roberto, D.; Tessore, F.; Ugo, R. *Coord. Chem. Rev.* **2006**, *250*, 1210.
(2) (a) Rosseinsky, M. J. *Microporous Mesoporous Mater.* **2004**, *73*, 15. (b) Kitagawa, S.; Kitaura, R.; Noro, S. *Angew. Chem., Int. Ed.* **2004**, *43*, 2334. (c) James, S. L. *Chem. Soc. Rev.* **2003**, *32*, 276.
(3) Maheswaran, S.; Chastanet, G.; Teat, S. J.; Mallah, T.; Sessoli, R.; Wernsdorfer, W.; Winpenny, R. E. P. *Angew. Chem., Int. Ed.* **2005**, *44*, 5044.
(4) Taylor, J. M.; Mahmoudkhani, A. H.; Shimizu, G. K. H. *Angew. Chem., Int. Ed.* **2007**, *46*, 795.
(5) Soghomonian, V.; Chen, Q.; Haushalter, R. C.; Zubieta, J. *Angew. Chem., Int. Ed. Engl.* **1995**, *34*, 223.
(6) Poojary, D. M.; Zhang, B.; Clearfield, A. *Chem. Mater.* **1999**, *11*, 421.
(7) Maeda, K.; Akimoto, J.; Kiyozumi, Y.; Mizukami, F. *Angew. Chem., Int. Ed. Engl.* **1995**, *34*, 1199.
(8) Clearfield, A. *Prog. Inorg. Chem.* **1998**, *47*, 371.
(9) Maeda, K.; Kiyozumi, Y.; Mizukami, F. *J. Phys. Chem. B.* **1997**, *101*, 4402.
(10) Odobel, F.; Bujoli, B.; Massiot, D. *Chem. Mater.* **2001**, *13*, 163.
(11) Alberti, G.; Casciola, M.; Costantino, U.; Peraio, A.; Montoneri, E. *Solid State Ionics* **1992**, *50*, 315.
(12) Alberti, G.; Casciola, M. *Solid State Ionics* **1997**, *97*, 177.
(13) Vermeulen, L. A.; Thompson, M. E. *Nature* **1992**, *358*, 656.
(14) Deniaud, D.; Schollorn, B.; Mansuy, D.; Rouxel, J.; Battioni, P.; Bujoli, B. *Chem. Mater.* **1995**, *7*, 995.
(15) Maillet, C.; Janvier, P.; Pipelier, M.; Praveen, T.; Andres, Y.; Bujoli, B. *Chem. Mater.* **2001**, *13*, 2879.

 Published on Web 02/18/2010

The structure adopted by metal phosphonates is dependent upon many factors such as the specific metal incorporated in the metal phosphonate; the shape, form, and protonation state of the phosphonic acid; the presence or absence of additional metal or organic cations; and synthesis parameters such as the solvothermal pressure-vessel fill volume, time of reaction, pH, temperature, solvent, and the presence or absence of any mineralizing agents.[16,17] To try to understand the structural consequences of some of the aforementioned factors we need systematic studies of the synthesis of these metal phosphonate materials in which, as far as possible, individual factors are varied one at a time. One of these factors is the structure of the phosphonic acid, of which the chain length of the organic group in an alkylenediphosphonic acid is a relatively easy parameter to vary. Research has shown that alkylenediphosphonic acids are versatile building units for the synthesis of hybrid materials, as certain homologues are commercially available, and others are relatively straightforward to synthesize. Simple modification of the structure of the alkylenediphosphonic acid by incrementally increasing the alkylene group chain length also provides the potential to modify the structure of the resultant material in a controlled fashion to enable certain structural features to be rationally designed, for instance, the pore height or inorganic layer separation.[8] Many studies have been reported in which the alkylene chain length of the diphosphonic acid has been varied from methylene to propylene,[18−20] with fewer having been continued to the butylene and pentylene chain lengths,[21] and still fewer to longer alkylene chain lengths.[16,22] Of these studies, it has been found that materials containing identical inorganic components have only been produced with a maximum of four successive $-CH_2-$ group chain length increases.[16] However, all such studies provide useful insight into the structural consequences of increasing the alkylene chain length in the synthesis of metal diphosphonates which will help to generate general synthesis pathways for the utilization of the organic components to form particular structural motifs in this complex family of materials.

We have been investigating the structural consequences of the effect of systematically increasing the length of the organic alkylene group within a diphosphonic acid on the resulting structure of group 13 metal alkylenediphosphonates. The group 13 metal alkylenediphosphonates are of potential interest because of their thermally stable and structurally diverse Al−O−P or Ga−O−P inorganic components that form the basis of the important family of microporous aluminum and gallium phosphate materials.[23] We have synthesized successfully a series of $Al_2[O_3PC_nH_{2n}PO_3](H_2O)_2F_2$ materials that all contain identical inorganic components and whose pore size and structure is systematically understood.[24−26] We have also synthesized the gallium-containing isostructural $n = 2$ member of the series that contains chains of GaO_4F_2 corner-sharing octahedra connected into a 3-dimensional framework structure by the ethylenediphosphonate groups in addition to gallium-containing methylendiphosphonates.[24,27,28] Currently other gallium ethylenediphosphonate materials have been reported[29], but no gallium diphosphonates with longer alkylene chains are known. In this work we report our efforts to investigate the structural consequences of increasing the alkylene group chain length in the diphosphonic acid component on neutral gallium diphosphonates synthesized from reaction gels containing the same chemical constituents and otherwise varying other factors as little as possible. The synthesis and structure of the three new gallium diphosphonates $Ga_3(OH)(O_3PC_3H_6PO_3)_2$ (**1**), $Ga_4(O_3PC_5H_{10}PO_3)_3(C_5H_5N)_2$ (**2**), and $Ga(HO_3PC_{10}H_{20}PO_3)$ (**3**) are reported, and the thermal properties of the framework material (**2**) are also presented. The variation of structure on the alkylene chain length is discussed and compared to other metal alkylenediphosphonate systems.

Experimental Section

Materials and Methods. The chemicals purchased to synthesize compounds **1**−**3** were $Ga_2(SO_4)_3 \cdot 18H_2O$ (Alfa-Aesar), HF (48.0 wt % in water, Aldrich), HF (70.0 wt % in pyridine, Aldrich), pyridine (Aldrich), ethanol (Aldrich), and 1,3-propylenediphosphonic acid (Alfa-Aesar). 1,5-Pentylenediphosphonic acid ($H_2O_3PC_5H_{10}PO_3H_2$) and 1,10-decylenediphosphonic acid ($H_2O_3PC_{10}H_{20}PO_3H_2$) were prepared according to literature methods.[21] All the reagents used to synthesize the pentylene- and decylenediphosphonic acids were obtained from Aldrich and, like the aforementioned reagents, were used without further purification.

Synthesis of $Ga_3(OH)(O_3PC_3H_6PO_3)_2$ (1). Compound **1** was prepared by mixing together gallium sulfate, 1,3-propylenediphosphonic acid, HF (70.0 wt % in pyridine, Aldrich), pyridine and deionized water to form a homogeneous reagent gel with a molar ratio of 1:2.05:4.12:25.4:68.3. The reagent mixture was loaded into 23 mL Teflon-lined steel autoclaves and heated for 4 days at 160 °C, under autogenous pressure. The initial and final pH values of the synthesis gel were 4.7 and 5.3, respectively. The white polycrystalline product was separated by suction filtration with a typical yield of ∼26%. Microprobe EDX analysis on the crystals indicated a Ga/P ratio of 3:4. Compound **1** was also prepared by mixing together gallium sulfate, 1,3-propylenediphosphonic acid and ethanol to form a homogeneous reagent gel with a molar ratio of 1:7.24:273. The reagent gel was loaded into 23 mL Teflon-lined steel autoclaves and heated for 7 days at 200 °C, under autogenous pressure. The initial and final pH values of the synthesis mixture were 0.4 and 2.8, respectively. The crystalline product was separated by suction filtration and had the form of small colorless single

(16) Ouellette, W.; Yu, M. H.; O'Connor, C. J.; Zubieta, J. *Inorg. Chem.* **2006**, *45*, 3224.
(17) Ouellette, W.; Yu, M. H.; O'Connor, C. J.; Zubieta, J. *Inorg. Chem.* **2006**, *45*, 7628.
(18) Serpaggi, F.; Ferey, G. *J. Mater. Chem.* **1998**, *8*, 2749.
(19) Distler, A.; Lohse, D. L.; Sevov, S. C. *J. Chem. Soc., Dalton Trans.* **1999**, 1805.
(20) Poojary, D. M.; Zhang, B.; Clearfield, A. *J. Am. Chem. Soc.* **1997**, *119*, 12550.
(21) Arnold, D. I.; Ouyang, X.; Clearfield, A. *Chem. Mater.* **2002**, *14*, 2020.
(22) Dines, M. D.; DiGiacomo, P. M.; Callahan, K. P.; Griffith, P. C.; Lane, R. H., Cooksey, R. E. In *Chemically Modified Surfaces in Catalysis and Electrocatalysis*; Miller, J. S., Ed.; American Chemical Society Symposium Series; American Chemical Society: Washington, DC, 1982; Vol. *192*, Chapter 12.
(23) Cheetham, A. K.; Ferey, G.; Loiseau, T. *Angew. Chem., Int. Ed.* **1999**, *38*, 3269.
(24) Harvey, H. G.; Teat, S. J.; Attfield, M. P. *J. Mater. Chem.* **2000**, *10*, 2632.
(25) Harvey, H. G.; Slater, B.; Attfield, M. P. *Chem.—Eur. J.* **2004**, *10*, 3270.
(26) Yuan, Z.; Clegg, W.; Attfield, M. P. *J. Porous Mater.* **2006**, *13*, 207.
(27) Attfield, M. P.; Harvey, H. G. *Mater. Res. Soc. Symp. Proc.* **2000**, *658*, GG6.31.1.
(28) Harvey, H. G.; Attfield, M. P. *Chem. Mater.* **2004**, *16*, 199.
(29) Bujoli-Doeuff, M.; Evain, M.; Janvier, P.; Massiot, D.; Clearfield, A.; Gan, Z.; Bujoli, B. *Inorg. Chem.* **2001**, *40*, 6694.

crystals. Microprobe EDX analysis on the crystals indicated a Ga/P ratio of 3:4.

Synthesis of $Ga_4(O_3PC_5H_{10}PO_3)_3(C_5H_5N)_2$ (2). Compound **2** was prepared by mixing together gallium sulfate, 1,5-pentylenediphosphonic acid, HF (48.0 wt % in water, Aldrich), pyridine and deionized water to form a homogeneous reagent gel with a molar ratio of 1:3.59:7.24:67.0:180. The reagent gel was loaded into 23 mL Teflon-lined steel autoclaves and heated for between 6 and 16 days at 190 °C. The initial and final pH values of the synthesis gel were 5.2 and 5.8, respectively. The crystalline products were separated by suction filtration and had the form of polycrystalline powders or small colorless single crystals, the latter being formed after 16 days of reaction. Typical yields for the reactions were ~40%. Microprobe EDX analysis on the crystals indicated a Ga/P ratio of 2:3.

Synthesis of $Ga(HO_3PC_{10}H_{20}PO_3)$ (3). Compound **3** was prepared by mixing together gallium sulfate, 1,10-decylenediphosphonic acid, HF (48.0 wt % in water, Aldrich), pyridine, and deionized water to form a homogeneous reagent gel with a molar ratio of 1:3.58:7.42:67.0:176. The reagent gel was loaded into 23 mL Teflon-lined steel autoclaves and heated for between 7 and 24 days at 190 °C. The initial and final pH values of the synthesis mixture were 5.5 and 5.9, respectively. The crystalline product was separated by suction filtration and had the form of small colorless single crystals with a typical yield of ~75%. Microprobe EDX analysis on the crystals indicated a Ga/P ratio of 1:2.

Thermogravimetric Analysis (TGA). TGA data were collected on a sample contained within an open alumina crucible using a Shimadzu TGA 50 under nitrogen flow from 20 to 800 °C at a heating rate of 10 °C min^{-1}.

Magic Angle Spinning Solid-State Nuclear Magnetic Resonance (MAS SS NMR). MAS SS NMR data were recorded using a Varian Unity Inova spectrometer with a 7.05 T Oxford Instruments magnet. Spectra collected for ^{31}P nuclei were referenced to an 85% solution of H_3PO_4 with the spectrometer operating at a frequency of 121.37 MHz, a sample spinning speed of 15.6 kHz, recycle delays of 300 s, and an acquisition time of 20.2 ms.

Powder X-ray Diffraction and Thermodiffraction. Laboratory powder X-ray diffraction (XRD) data were collected using a Phillips X'Pert Pro diffractometer using graphite-monochromated Cu−Kα_{1+2} radiation, with a scan step size of 0.033° 2θ and a counting time of 0.5 s per step in the range 5−50, 3−60, and 4−45° 2θ for compounds **1**, **2**, **3**, respectively. Synchrotron X-ray data were collected on a sample of **1** synthesized in the HF/pyridine solvent system contained in a 0.5 mm diameter Lindemann glass capillary tube mounted on the high-resolution X-ray diffractometer at station 2.3, Daresbury SRS, U.K. The incident X-ray wavelength was 1.25078 Å, selected using an Si(111) monochromator. Data were collected in steps of 0.01° 2θ, with a collection time per step of 3 s between 3.5 and 20° 2θ, 6 s between 20 and 50° 2θ, 12 s between 50 and 80° 2θ, and 20 s between 80 and 84.51° 2θ. A LeBail fit[30] to the diffraction data for samples **1** synthesized in the HF/pyridine solvent system and **3** were performed using the GSAS suite of programs.[31] Thermodiffraction patterns for compound **2** were collected using a Panalytical X'Pert Pro diffractometer in reflection geometry employing Cu−Kα radiation and an RTMS X'Celerator detector, fitted with an Anton Paar XRK 900 high-temperature furnace stage. The sample was heated, under vacuum, from 35 to 710 °C at a heating rate of 10 °C min^{-1}, with patterns being collect at 30 °C intervals. The XRD patterns were all collected in the 3−60° 2θ range with a scan time of 15 min per scan.

Single-Crystal Structure Determination of Compounds 1, 2, and 3. Single-crystal X-ray data were collected from colorless crystals of compounds **1** and **2** mounted on a Nonius Kappa-CCD diffractometer fitted with a sealed Mo−Kα X-ray tube, and from a colorless crystal of compound **3** mounted on a Bruker-Nonius APEXII CCD diffractometer at the high-flux single-crystal diffraction station 9.8, Daresbury Laboratory Synchrotron Radiation Source, U.K. Absorption corrections were applied based on symmetry-equivalent and repeated reflections.

The structures were determined by direct methods and refined by full-matrix least-squares on F^2 using the SHELXTL suite of programs.[32] The crystals of **2** were nonmerohedrally twinned, preventing the merging of equivalent reflections before refinement and requiring application of nonmerohedral twin laws to the original diffraction data before a satisfactory refinement resulted.[33] The gallium and phosphorus atom positions were determined directly from the structure solution, and all the non-hydrogen atoms were located subsequently from difference Fourier maps. The atomic displacement parameters of all non-hydrogen atoms were refined anisotropically. All the hydrogen atoms of the alkylene linker groups were positioned geometrically and refined in riding mode with their isotropic atomic displacement parameters fixed at 1.2 times the equivalent isotropic atomic displacement parameter of the carbon atoms to which they were directly connected. The hydrogen atom of the hydroxyl group in compound **1** was not located in a difference Fourier map and could not be positioned geometrically with confidence. The hydrogen atoms of the pyridine molecules in compound **2** were positioned geometrically and refined in riding mode with their isotropic atomic displacement parameters fixed at 1.2 times the equivalent isotropic atomic displacement parameter of the carbon atoms to which they were directly connected. The hydrogen atom of the P−O−H group in compound **3** was located in a difference Fourier map, and its isotropic atomic displacement parameter was fixed at 1.2 times the equivalent isotropic atomic displacement parameter of the oxygen atom. For the non-centrosymmetric structures of **1** and **2** an absolute structure parameter was refined;[34] in the case of **1** the crystal was found to be an inversion twin. The crystallographic data and structure refinement parameters for compounds **1**, **2**, and **3** are given in Table 1, selected bond distances and angles are presented in Tables 2, 3, and 4, and hydrogen bond geometry for compound **3** is presented in Table 5.

Results and Discussion

$Ga_3(OH)(O_3PC_3H_6PO_3)_2$ (1). The powder XRD patterns of **1** synthesized in different solvent systems are provided in the Supporting Information (Figures S1 and S2). The Le Bail profile fitting analysis on the polycrystalline sample of **1** prepared in the HF/pyridine solvent system indicated the sample was monophasic and yielded the lattice parameters a = 38.0086(4) Å, b = 9.99995(9) Å, c = 8.31916(7) Å. The latter are in excellent agreement with the lattice parameters obtained from the single-crystal structure (see Table 1), indicating that the same phase has been synthesized from different solvent systems. The sample of **1** prepared in ethanol was judged to be monophasic from the excellent agreement between the observed powder XRD patterns and that calculated using the single-crystal structure of the material.

The structure of **1** is shown in Figure 1. The main structural features of **1** are the 2-dimensional slabs of

(30) Le Bail, A.; Duroy, H.; Fourquet, J. *Mater. Res. Bull.* **1988**, *23*, 447.
(31) Von Dreele, R. B.; Larson, A. C. *GSAS, General Structure Analysis System*; Regents of the University of California: LANSCE, Los Alamos National Laboratory: Los Alamos, NM, 1995.
(32) Sheldrick, G. M. *Acta Crystallogr., Sect. A* **2008**, *64*, 112.
(33) Spek, A. L. *J. Appl. Crystallogr.* **2003**, *36*, 7.
(34) Flack, H. D. *Acta Crystallogr., Sect. A* **1983**, *39*, 876.

Table 1. Crystal Data and Structure Refinement Parameters for **1**, **2**, and **3**

formula	$C_6H_{13}Ga_3O_{13}P_4$	$C_{25}H_{40}Ga_4N_2O_{18}P_6$	$C_{20}H_{42}Ga_2O_{12}P_4$
formula weight	626.2	1121.3	737.9
temperature (K)	150	150	120
wavelength (Å)	0.71073	0.71073	0.6902
crystal system	orthorhombic	monoclinic	monoclinic
space group	$Cmc2_1$	$P2_1$	$C2/c$
a (Å)	37.990(8)	9.6394(19)	34.794(6)
b (Å)	10.022(2)	8.3158(16)	4.8924(9)
c (Å)	8.3093(17)	22.717(5)	17.454(3)
β (deg)		93.117(3)	104.425(3)
V (Å^3)	3163.6(11)	1818.3(6)	2877.5(9)
Z	8	2	4
D_c (g cm^{-3})	2.629	2.048	1.703
μ (mm^{-1})	5.548	3.277	2.153
crystal size (mm)	0.10 × 0.05 × 0.01	0.10 × 0.05 × 0.02	0.12 × 0.03 × 0.02
transmission	0.589−0.944	0.825−0.937	0.772−0.958
reflns measd	5939	13169	14120
unique reflns, R_{int}	2504, 0.0570	13169	4177, 0.0576
refined parameters	165	503	177
goodness-of-fit[a]	1.062	1.077	1.026
R (F, $F^2 > 2\sigma$)[b]	0.0495	0.0376	0.0388
R_w (F^2, all data)[c]	0.0962	0.1046	0.0997
absolute structure parameter	0.46(2)	0.050(10)	
max, min el dens (e Å^{-3})	0.92, −0.90	1.00, −0.84	0.91, −0.93

[a] Goodness-of-fit = $\{\sum[w(F_o^2 - F_c^2)^2]/(\text{no. of data} - \text{no. of params})\}^{1/2}$. [b] $R = \sum||F_o| - |F_c||/\sum|F_o|$. [c] $R_w = \{\sum w(F_o^2 - F_c^2)^2/\sum w(F_o^2)^2\}^{1/2}$.

Table 2. Selected Bond Distances (Å) and Angles (deg) for **1**[a]

Ga1−O3	1.921(7)	Ga1−O4	1.923(7)
Ga1−O2	1.960(7)	Ga1−O13	1.964(7)
Ga1−O5[b]	1.999(7)	Ga1−O1	2.006(7)
Ga2−O7	1.818(7)	Ga2−O6	1.818(7)
Ga2−O9	1.822(7)	Ga2−O8[c]	1.826(6)
Ga3−O11[d]	1.801(7)	Ga3−O13	1.816(7)
Ga3−O10[b]	1.828(7)	Ga3−O12	1.856(7)
P1−O3[e]	1.512(7)	P1−O7	1.533(7)
P1−O8	1.552(7)	P1−C1	1.816(10)
P2−O5	1.518(7)	P2−O4	1.525(7)
P2−O6	1.551(7)	P2−C3	1.770(10)
P3−O1	1.503(7)	P3−O9	1.559(8)
P3−O10	1.560(7)	P3−C5	1.785(10)
P4−O2	1.502(7)	P4−O12	1.552(7)
P4−O11	1.552(7)	P4−C7	1.798(11)
O3−Ga1−O4	94.2(3)	O3−Ga1−O2	90.1(3)
O4−Ga1−O2	172.8(3)	O3−Ga1−O13	173.2(3)
O4−Ga1−O13	88.9(3)	O2−Ga1−O13	87.5(3)
O3−Ga1−O5[b]	96.6(3)	O4−Ga1−O5[b]	90.7(3)
O2−Ga1−O5[b]	83.0(3)	O13−Ga1−O5[b]	89.4(3)
O3−Ga1−O1	84.9(3)	O4−Ga1−O1	96.0(3)
O2−Ga1−O1	90.2(3)	O13−Ga1−O1	88.8(3)
O5[b]−Ga1−O1	173.0(3)		
O7−Ga2−O6	99.6(3)	O7−Ga2−O9	119.4(3)
O6−Ga2−O9	109.8(3)	O7−Ga2−O8[c]	106.0(3)
O6−Ga2−O8[c]	113.0(3)	O9−Ga2−O8[c]	108.9(3)
O11[d]−Ga3−O13	119.6(3)	O11[d]−Ga3−O10[b]	107.6(3)
O13−Ga3−O10[b]	105.0(3)	O11[d]−Ga3−O12	109.0(3)
O13−Ga3−O12	110.3(3)	O10[b]−Ga3−O12	104.1(3)

[a] The symmetry transformations used to generate equivalent atoms are given in the following footnotes. [b] $x, -y, z-1/2$. [c] $x, -y-1, z-1/2$. [d] $x, -y, z+1/2$. [e] $x, y, z+1$.

18.0 Å thickness that are themselves constructed from two thinner 7.8 Å Ga−P−O/OH/CH hybrid layers connected together on one side only by the propylene chains of the diphosphonate ligand.

The 7.8 Å thick Ga−P−O/OH/CH hybrid layers contain $Ga1O_5(OH)$ octahedra, and $Ga3O_3(OH)$ and $Ga2O_4$ tetrahedra. Each $Ga1O_5(OH)$ octahedron and $Ga3O_3$-(OH) tetrahedon share one common vertex, the O13 hydroxyl group, to form a dinuclear unit of Ga-centered polyhedra. All the dinuclear units of Ga-centered polyhedra and mononuclear GaO_4 tetrahedra are connected together by individual phosphonate $-PO_3$ groups through Ga−O−P bonds with Ga1, Ga2, and Ga3 being bound to five, four, and three individual $-PO_3$ groups respectively. Each 7.8 Å thick Ga−P−O/OH/CH hybrid layer itself consists of a layer of $Ga1O_5(OH)$, $Ga2O_4$, $CP1O_3$, and $CP2O_3$ polyhedra connected to a layer of $Ga3O_3(OH)$, $CP3O_3$, and $CP4O_3$ polyhedra. The $CP1O_3$ and $CP2O_3$ tetrahedra of the former layer form the bases of the pillars to the adjacent 7.8 Å thick Ga−P−O/OH/CH hybrid layer, as shown in Figure 1b. The $CP3O_3$ and $CP4O_3$ tetrahedra of the latter layer of the 7.8 Å thick Ga−P−O/OH/CH hybrid layer are connected by the propylene groups so that this layer contains a complete diphosphonate group, as shown in Figure 1c, which is oriented orthogonally to those that pillar the two adjacent 7.8 Å thick Ga−P−O/OH/CH hybrid layers. The ^{31}P MAS SS NMR spectrum of the material contains four resonances in the range 10−36 ppm as seen in Figure 2. This result is consistent with the four crystallographically independent phosphorus sites belonging to the three structurally independent diphosphonate groups in the structure, and the chemical shift values are similar to those observed in other gallium phosphonates.[35,36]

Formation of the 18.0 Å thick 2-dimensional slabs that each contain pillared 7.8 Å thick Ga−P−O/OH/CH hybrid layers and the presence of diphosphonate groups in the outer layers of these 7.8 Å thick Ga−P−O/OH/CH hybrid layers that are orthogonal to the diphosphonate groups pillaring the 7.8 Å thick Ga−P−O/OH/CH hybrid layers are an uncommon arrangement in metal phosphonate chemistry. The former feature has been reported in other compounds.[16,17,37] The 18.0 Å thick

(35) Attfield, M. P.; Harvey, H. G.; Teat, S. J. *J. Solid State Chem.* **2004**, *177*, 2951.
(36) Harvey, H. G.; Herve, A. C.; Hailes, H. C.; Attfield, M. P. *Chem. Mater.* **2004**, *16*, 3756.
(37) Bonavia, G. H.; Haushalter, R. C.; Lu, S.; O'Connor, C. J.; Zubieta, J. *J. Solid State Chem.* **1997**, *132*, 144.

Table 3. Selected Bond Distances (Å) and Angles (deg) for **2**[a]

Ga1−O6	1.799(3)	Ga1−O15[b]	1.799(3)
Ga1−O14	1.811(3)	Ga1−O5	1.823(4)
Ga2−O10	1.798(3)	Ga2−O3	1.803(3)
Ga2−O2	1.808(3)	Ga2−O12	1.815(3)
Ga3−O13[c]	1.920(3)	Ga3−O18	1.930(3)
Ga3−O11	1.961(3)	Ga3−O17	1.977(3)
Ga3−O16	1.978(3)	Ga3−N1	2.080(4)
Ga4−O9	1.933(4)	Ga4−O4	1.938(3)
Ga4−O8	1.953(3)	Ga4−O7	1.958(3)
Ga4−O1[d]	1.974(3)	Ga4−N2	2.107(4)
P1−O8	1.509(4)	P1−O13	1.518(3)
P1−O6	1.544(3)	P1−C1	1.794(5)
P2−O17[e]	1.505(3)	P2−O12[d]	1.536(3)
P2−O5	1.547(4)	P2−C5	1.778(5)
P3−O1	1.511(3)	P3−O14[f]	1.544(3)
P3−O2	1.548(3)	P3−C7	1.790(5)
P4−O4[c]	1.498(3)	P4−O16	1.515(4)
P4−O3[c]	1.565(3)	P4−C10	1.790(5)
P5−O18	1.509(3)	P5−O7	1.516(3)
P5−O15	1.565(3)	P5−C13	1.802(5)
P6−O11	1.499(4)	P6−O9	1.507(4)
P6−O10	1.541(3)	P6−C15	1.800(5)
O6−Ga1−O15[b]	110.74(15)	O6−Ga1−O14	108.10(15)
O15[b]−Ga1−O14	114.66(15)	O6−Ga1−O5	105.33(15)
O15[b]−Ga1−O5	113.76(16)	O14−Ga1−O5	103.57(15)
O10−Ga2−O3	111.52(15)	O10−Ga2−O2	105.17(15)
O3−Ga2−O2	112.81(15)	O10−Ga2−O12	108.79(15)
O3−Ga2−O12	113.81(15)	O2−Ga2−O12	104.13(15)
O13[c]−Ga3−O18	98.70(14)	O13[c]−Ga3−O11	97.80(14)
O18−Ga3−O11	90.10(15)	O13[c]−Ga3−O17	88.05(14)
O18−Ga3−O17	172.94(15)	O11−Ga3−O17	86.93(14)
O13[c]−Ga3−O16	89.07(14)	O18−Ga3−O16	90.20(15)
O11−Ga3−O16	173.00(14)	O17−Ga3−O16	91.98(14)
O13[c]−Ga3−N1	168.06(15)	O18−Ga3−N1	90.63(15)
O11−Ga3−N1	89.57(16)	O17−Ga3−N1	82.95(15)
O16−Ga3−N1	83.43(15)		
O9−Ga4−O4	99.10(15)	O9−Ga4−O8	97.30(15)
O4−Ga4−O8	91.41(15)	O9−Ga4−O7	89.04(15)
O4−Ga4−O7	89.73(15)	O8−Ga4−O7	173.30(14)
O9−Ga4−O1[d]	88.36(14)	O4−Ga4−O1[d]	172.44(15)
O8−Ga4−O1[d]	86.37(14)	O7−Ga4−O1[d]	91.66(14)
O9−Ga4−N2	168.07(15)	O4−Ga4−N2	90.82(15)
O8−Ga4−N2	89.01(15)	O7−Ga4−N2	84.36(15)
O1[d]−Ga4−N2	81.92(14)		

[a] The symmetry transformations used to generate equivalent atoms are given in the following footnotes. [b] $x, y+1, z$. [c] $x, y-1, z$. [d] $x-1, y, z$. [e] $x-1, y+1, z$. [f] $x+1, y-1, z$.

2-dimensional slabs are stacked along the *a* axis in such a manner that they are displaced with respect to each other in the *bc* planes. The neutral layers are held together by weak hydrogen-bond C−H···O type interactions between the propylene chain hydrogen atoms on one 18.0 Å thick 2-dimensional slab and the oxygen atoms in the adjacent 18.0 Å thick 2-dimensional slab. The alignment of these hydrogen-bonding interactions causes the displacement of adjacent 18.0 Å thick 2-dimensional slabs with respect to each other in the *bc* planes as seen in Figure 1b. The pillars within the 18.0 Å thick 2-dimensional layers are too close to one another to allow any non-framework species to be present within this region.

$Ga_4(O_3PC_5H_{10}PO_3)_3(C_5H_5N)_2$ (2). The powder XRD pattern of **2** is provided in the Supporting Information (Figure S3) and was judged to be essentially monophasic from the good agreement between the observed powder XRD pattern and that calculated using the single-crystal structure of the material. There are traces of other unidentified minor phases in the observed powder XRD pattern.

Table 4. Selected Bond Distances (Å) and Angles (deg) for **3**[a]

Ga1−O1[b]	1.944(2)	Ga1−O1[c]	1.944(2)
Ga1−O3[d]	1.943(2)	Ga1−O3[e]	1.943(2)
Ga1−O6	1.976(2)	Ga1−O6[f]	1.976(2)
Ga2−O2[g]	1.796(2)	Ga2−O2[c]	1.796(2)
Ga2−O5	1.822(2)	Ga2−O5[h]	1.822(2)
P1−O1	1.512(2)	P1−O2	1.535(2)
P1−O3	1.519(2)	P1−C1	1.785(3)
P2−O4	1.564(2)	P2−O5	1.522(2)
P2−O6	1.507(2)	P2−C10	1.776(3)
O1[b]−Ga1−O1[c]	180	O1[b]−Ga1−O3[d]	91.14(7)
O1[b]−Ga1−O3[e]	88.86(7)	O1[c]−Ga1−O3[d]	88.86(7)
O1[c]−Ga1−O3[e]	91.14(7)	O1[b]−Ga1−O6	88.67(7)
O1[c]−Ga1−O6	91.33(7)	O1[b]−Ga1−O6[f]	91.33(7)
O1[c]−Ga1−O6[f]	88.67(7)	O3[d]−Ga1−O3[e]	180
O3[d]−Ga1−O6	90.98(7)	O3[e]−Ga1−O6	89.02(7)
O3[d]−Ga1−O6[f]	89.02(7)	O3[e]−Ga1−O6[f]	90.98(7)
O6−Ga1−O6[f]	180		
O2[g]−Ga2−O2[c]	106.3(1)	O2[g]−Ga2−O5	102.77(9)
O2[c]−Ga2−O5	117.11(8)	O2[g]−Ga2-O5[h]	117.11(8)
O2[c]−Ga2-O5[h]	102.77(9)	O5−Ga2−O5[h]	111.3(1)

[a] The symmetry transformations used to generate equivalent atoms are given in the following footnotes. [b] $-x+3/2, y-1/2, -z-1/2$. [c] $x+1/2, -y+5/2, z+1/2$. [d] $-x+3/2, y+1/2, -z-1/2$. [e] $x+1/2, -y+3/2, z+1/2$. [f] $-x+2, -y+2, -z$. [g] $-x+3/2, -y+5/2, -z$. [h] $-x+2, y, -z+1/2$.

Table 5. Hydrogen Bond Donor−acceptor Distances (Å) and Angles (deg) for **3**[a]

D−H···A	D−H	H···A	D···A	D−H···A
O4−H4···O3[b]	0.75(3)	2.01(3)	2.681(3)	148(4)
O4−H4···O6[c]	0.75(3)	2.48(4)	2.887(2)	116(3)

[a] The symmetry transformations used to generate equivalent atoms are given in the following footnotes. [b] $x+1/2, -y+3/2, z+1/2$. [c] $x, y-1, z$.

The structure of $Ga_4(O_3PC_5H_{10}PO_3)_3(C_5H_5N)_2$ (**2**) is shown in Figure 3 and consists of Ga−P−O layers connected together on both sides by the pentylene chains of the diphosphonate ligand to produce a 3-dimensional framework structure. The Ga−P−O layers consist of GaO_5N octahedra, GaO_4 tetrahedra, and CPO_3 tetrahedra. All the GaO_5N octahedra and GaO_4 tetrahedra are connected together by individual phosphonate $-PO_3$ groups through Ga−O−P bonds, with the GaO_5N octahedra and GaO_4 tetrahedra being bound to five and four individual $-PO_3$ groups, respectively. The diphosphonate groups provide all the oxygen atoms of the Ga-centered polyhedra. The sixth coordination site of the GaO_5N octahedron, the nitrogen atom, is donated by a neutral pyridine molecule which was introduced into the synthetic system as a co-solvent. Similar coordination of pyridine to Ga^{3+} cations has been observed in other gallium diphosphonate materials.[38] The GaO_5N octahedra are arranged within a Ga−P−O layer so that all the pyridine molecules protrude in one direction only, and within the structure the Ga−P−O layers are stacked so that the pyridine molecules of alternate layers are directed in opposite directions, as seen in Figure 3b. This stacking arrangement of the Ga−P−O layers results in two types of interlayer regions being formed. The first contains pentylene linker groups only, and these are too close to one another to allow any non-framework species to be present within this region. The second type of interlayer region contains pentylene linker groups and the pyridine molecules and can be considered to contain a

(38) Yuan, Z.; Clegg, W.; Attfield, M. P. *J. Solid State Chem.* **2006**, *179*, 1739.

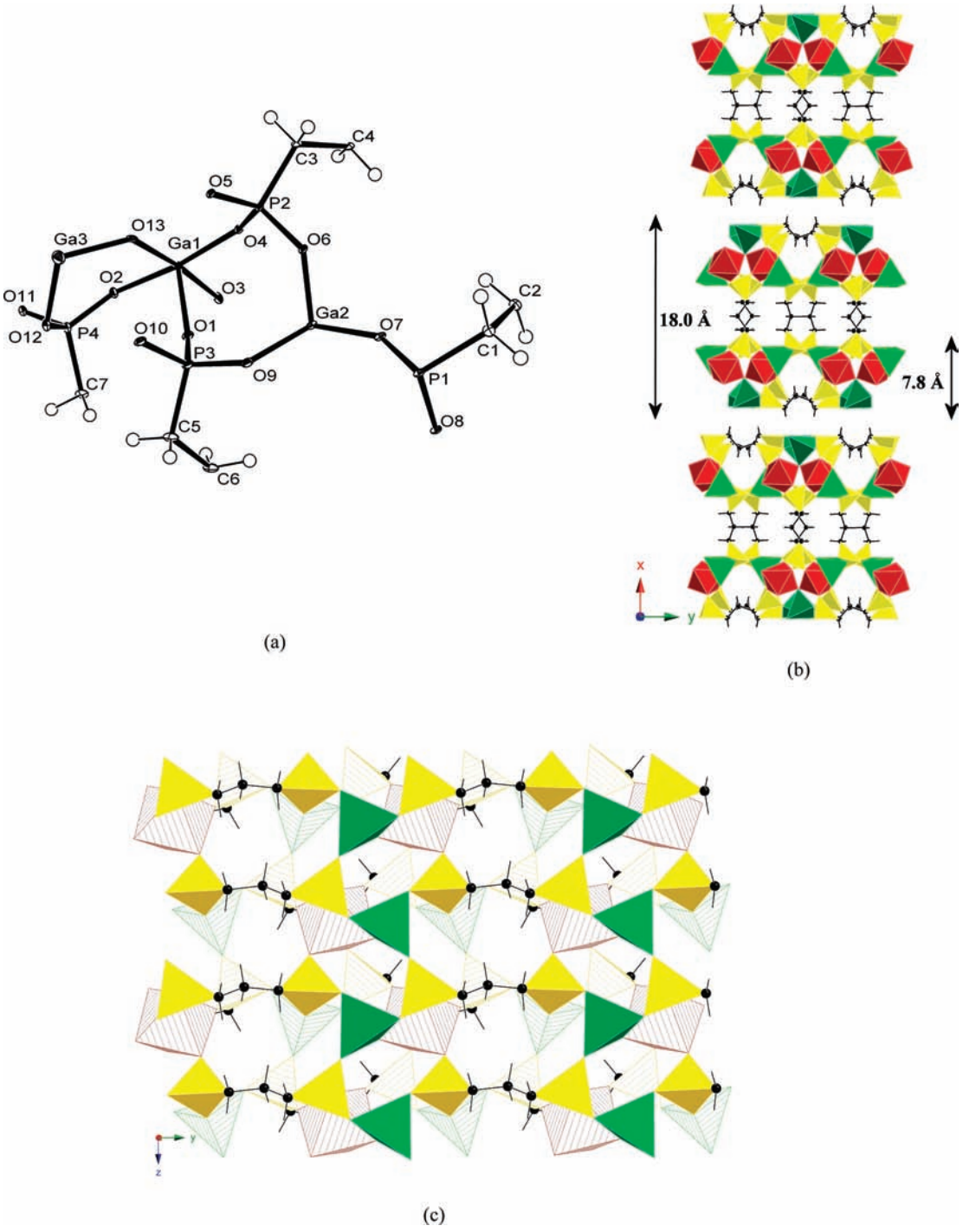

Figure 1. (a) Asymmetric unit of $Ga_3(OH)(O_3PC_3H_6PO_3)_2$ (**1**) with anisotropic atomic displacement ellipsoids shown at the 50% probability level. (b) A polyhedral/ball-and-stick representation of **1** viewed along the *c* axis. (c) A polyhedral/ball-and-stick representation of the 7.8 Å thick Ga−P−O/OH/CH hybrid layer viewed along the *a* axis. Key: octahedral GaO_6 red, tetrahedral $GaO_3(OH)$ dark green, tetrahedral GaO_4 light green, tetrahedral PCO_3 yellow, carbon black spheres, hydrogen small gray spheres. The hatched polyhedra in (c) are in the layer below the fully shaded polyhedra.

one-dimensional channel system in which the channels run parallel to the [010] direction. The channels are bounded by rings of 10 polyhedra and the pentylene chains of the diphosphonate groups, which results in channel surfaces containing both hydrophobic and hydrophilic portions. The channels are occupied by the pyridine molecules that are directly coordinated to the Ga3/4 atoms within the framework. The pyridine molecules can be thought of as forming part of the framework structure, as other molecules, for example, water, commonly do in framework materials.[24−26] However, the size of the pyridine molecule leads to these molecules simultaneously acting in a structure-directing capacity, as their presence forces the framework to develop around their large bulk. Thus, the bound pyridine molecules act in a spacing-filling mode to direct the formation of the framework structure within this material.

The ^{31}P MAS SS NMR spectrum of the material is shown in Figure 4 and shows four resonances at 4.9, 12.6, 17.6, and 18.7 ppm. These chemical shift values are

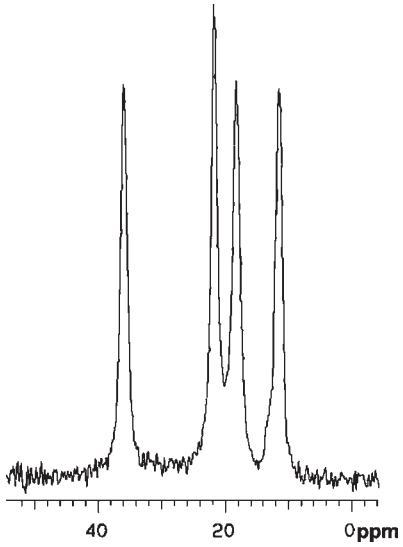

Figure 2. ^{31}P solid-state MAS NMR spectrum of **1**.

similar to those observed in other gallium phosphonates.[35,36] This result is apparently inconsistent with the six crystallographically independent phosphorus sites belonging to the three structurally independent diphosphonate groups in the structure. However, the peaks at 4.9 and 12.6 ppm are both slightly asymmetric and broader than those at 17.6 and 18.7 ppm, indicating that the former are probably both unresolved pairs, which results in there being six crystallographically independent phosphorus sites in agreement with the crystallographically determined structure.

The thermal behavior of compound **2** was fully investigated, as the presence of relatively weakly coordinated pyridine molecules within the framework structure indicated that the material could potentially exhibit microporosity. The TGA trace for compound **2** is shown in Figure 5 and displays a rapid mass loss of 5% between 190 and 250 °C, a second more gradual mass loss of 3.5% between 250 and 430 °C, a third rapid mass loss of 5% between 450 and 500 °C, and a final mass loss of 3.4% between 500 and 720 °C. The first three mass losses (total 13.0%) are attributed to the loss of the pyridine molecules (calculated 14.1%), which appears to occur in two main stages at 225 and 460 °C, indicating that a total of one pyridine molecule is lost during each step. The final mass loss is attributed to the incomplete decomposition of the organic portion of the pentylenediphosphonate groups (calculated 19% for complete decomposition). Such incomplete decomposition of the alkylene chains of group 13 metal diphosphonates when heated under a nitrogen atmosphere has been observed previously.[25,36]

The thermodiffraction data of compound **2** are shown in Figure 6. From 35 up to 230 °C there are only minor changes in the diffraction peak positions, but the intensity of the (002) peak is seen to decrease. By 230 °C a new low angle peak at ~9° 2θ has developed which is adjacent to the original (002) peak. As the temperature is raised from 230 °C the (002) peak is seen to decrease in intensity and the peak at ~9° 2θ is seen to increase in intensity up to 440 °C before the intensity begins to decrease. The peak at ~9° 2θ disappears by 470 °C, and the (002) peak disappears by 500 °C. Above 500 °C the few remaining diffraction peaks rapidly diminish until at 710 °C the material becomes X-ray amorphous.

The combination of the thermogravimetric and thermodiffraction data suggests that the framework structure of $Ga_4(O_3PC_5H_{10}PO_3)_3(C_5H_5N)_2$ (**2**) remains stable with respect to the loss of one pyridine molecule from the intralayer region. Upon loss of this first pyridine molecule the material of approximate formula $Ga_4(O_3PC_5H_{10}PO_3)_3(C_5H_5N)$ undergoes some structural rearrangement, producing a slightly modified diffraction pattern compared to the original. The $Ga_4(O_3PC_5H_{10}PO_3)_3(C_5H_5N)$ material remains stable until 470 °C when the second pyridine molecule is all removed, at which point the peak at ~9° 2θ disappears. The (002) peak then decreases and disappears by ~530 °C, which corresponds to the collapse of the diphosphonate pillars. Hence, the framework of compound **2** is stable with respect to loss of 1 equiv of pyridine molecules but collapses rapidly when the second equivalent of pyridine molecules is removed, collapsing completely upon decomposition of the diphosphonate linkers.

The solvent-accessible volume of the pores containing the pyridine molecules in **2** calculated using SQUEEZE[33,39] in the absence of the pyridine molecules was 409 Å^3. However, nitrogen adsorption experiments performed on a sample degassed overnight at 473 K showed no significant adsorption of nitrogen into the internal volume of the material.

$Ga(HO_3PC_{10}H_{20}PO_3)$ (3). The powder XRD pattern of **3** is provided in the Supporting Information (Figure S4). The Le Bail profile fitting analysis on the polycrystalline sample of **3** indicated the sample was essentially monophasic, with only traces of other unidentified minor phases present.

The structure of $Ga(HO_3PC_{10}H_{20}PO_3)$ (**3**) is shown in Figure 7 and consists of Ga−P−O layers connected together on both sides by the decylene chains of the diphosphonate ligands to produce a 3-dimensional pillared structure. The Ga−P−O layers consist of $Ga1O_6$ octahedra, $Ga2O_4$ tetrahedra and CPO_3 tetrahedra. All the GaO_6 octahedra and GaO_4 tetrahedra are connected together by phosphonate $-PO_3$ groups through Ga−O−P bonds, with the GaO_6 octahedra and GaO_4 tetrahedra being bound to six and four individual $-PO_3$ groups respectively. The Ga−P−O layers contain rows of GaO_4 tetrahedra and rows of GaO_6 octahedra separated by rows of CPO_3 tetrahedra as shown in Figure 7c. The diphosphonate groups provide all the oxygen atoms of the Ga-centered polyhedra. One oxygen atom, O4, of the diphosphonate group remains protonated as a pendant −P−O−H group [P2−O4 1.564(2) Å] and is hydrogen bonded to two other oxygen atoms of the phosphonate groups, O3 and O6 (Table 5). The ^{31}P MAS SS NMR spectrum of the material contains two resonances at 14.78 and 28.76 ppm as seen in Figure 8. This result is consistent with the two crystallographically independent phosphorus sites in the structure, and the chemical shift values are similar to those observed in other gallium phosphonates.[35,36] The interlayer regions contain the decylene linker groups, which are too close to one

(39) Sluis, P. V. D.; Spek, A. L. *Acta Crystallogr., Sect. A* **1990**, *46*, 194.

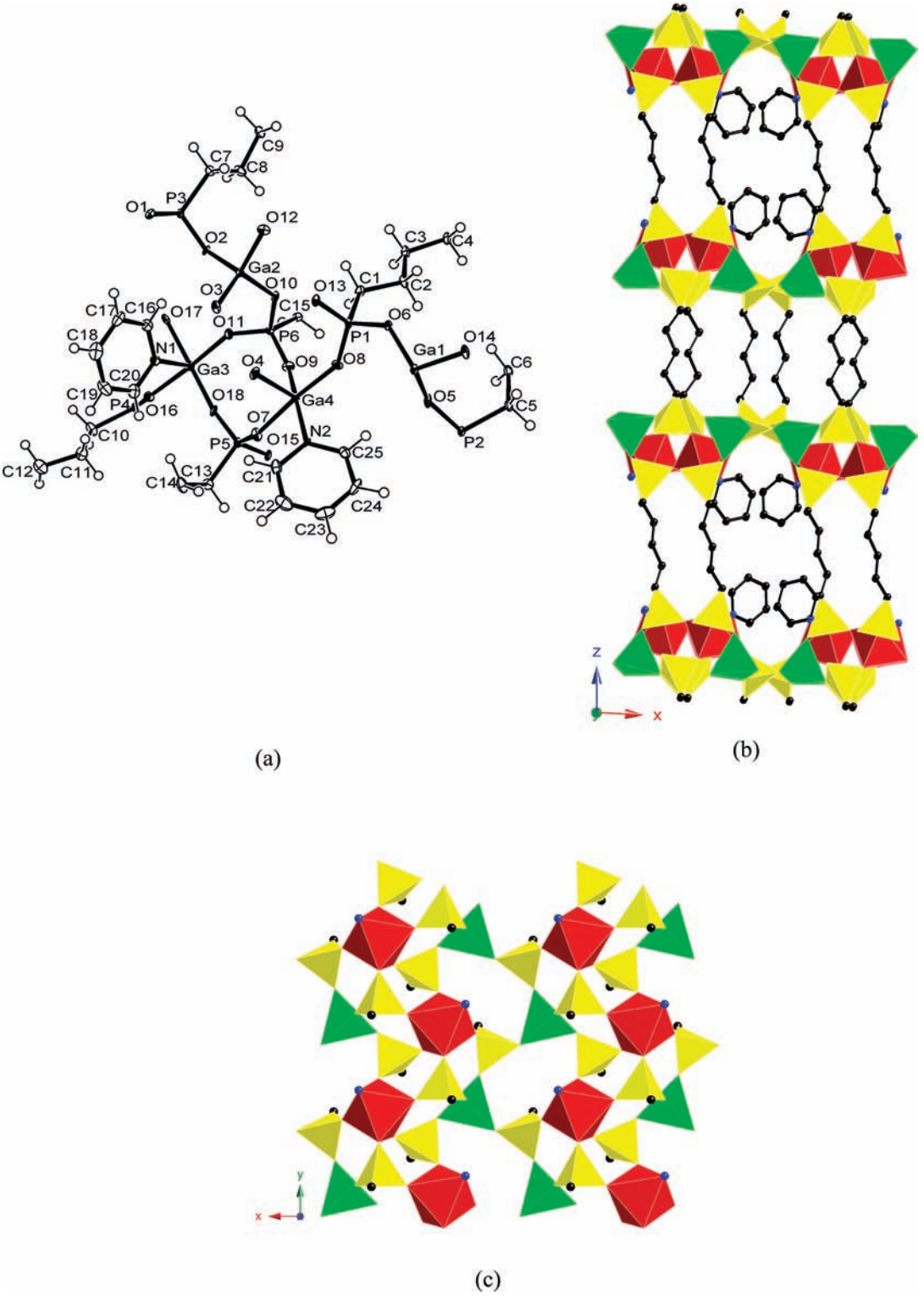

Figure 3. (a) Asymmetric unit of $Ga_4(O_3PC_5H_{10}PO_3)_3(C_5H_5N)_2$ (**2**) with anisotropic atomic displacement ellipsoids shown at the 50% probability level. (b) A polyhedral/ball-and-stick representation of **2** viewed along the *b* axis. (c) A polyhedral/ball-and-stick representation of the Ga−P−O hybrid layer viewed along the *c* axis. Key: octahedral $GaNO_5$ red, tetrahedral GaO_4 light green, tetrahedral PCO_3 yellow, carbon black spheres, nitrogen blue spheres. Hydrogen atoms have been omitted from (b) and (c) for clarity.

another to allow any non-framework species to be present within this region.

We have now synthesized and structurally characterized six gallium alkylenediphosphonate materials from synthesis gels that contain the identical components of gallium sulfate, the appropriate alkylenediphosphonic acid, pyridine, HF, and water in which the alkylene chain of the diphosphonic acid contains one, two, three, five, or ten $-CH_2-$ groups. Comparison of the structures of the products formed as the alkylene linker component of the diphosphonic acid increases provides some general approaches to prepare certain structural types within this

system. In addition, comparison to other similar studies where a range of metal diphosphonates has been prepared under similar conditions and the alkylene spacer length of the diphosphonic acid has been increased systematically is also instructive to allow broader strategies of structure design in metal diphosphonates as a whole to be developed.

All the gallium diphosphonate materials produced from these synthetic gels contain a pillared-type layer motif except for $(C_5H_5NH)[Ga_2(H_2O)_2(O_3PCH_2PO_3)(O_3PCH_2PO_3H)]$ and $(C_5H_5NH)[Ga(H_2O)(O_3PCH_2PO_3)]$[28] in which the short spacer length ($-CH_2-$) of the diphosphonic acid favors coordination to one gallium cation through both $-PO_3$ groups, precluding pillaring to adjacent Ga−P−O layers. This behavior has been reported in many other metal methylenediphosphonates,[19,40−42] although pillaring behavior is found in some compounds, for example lanthanide methylenediphosphonates.[18] Increasing the alkylene chain in the diphosphonic acid to ethylene provides the correct spacer length to allow the predominant formation of pillared materials. This is exemplified in the formation of $Ga_2[O_3PC_2H_4PO_3](H_2O)_2F_2\cdot H_2O$,[24,27] a pillared material in which there is enough spacing between adjacent organic pillars to accommodate extra-framework water molecules, and is also observed in other metal diphosphonate systems.[16,19,20,24] Increasing the chain length $(-CH_2-)_n$ to $n = 3$, 5, and 10 results in formation of pillared materials, but of two different types. For $n = 3$ the material contains 2-dimensional pillared slabs in which the organic tether projects from one side of each Ga−P−O/OH hybrid layer only, as seen in Figure 2b. Increasing the alkylene chain length further to $n = 5$ or 10 results in the formation of pillared materials that contain organic tethers projecting from both sides of each Ga−P−O layer as seen in Figure 3 and 7. A similar trend has been reported for neutral oxovanadium diphosphonate compounds,[16] although the transitions from compounds with a fully pillared structure to compounds containing pillared slabs back to fully pillared structures occurs at different lengths of the alkylene linking group. This type of transition between fully pillared structures−pillared slab structures−fully pillared structures may be a general trend within series of metal alkylenediphosphonate materials but requires more studies for different metal species to be verified. One definite variation that can be ascertained from this and other studies is that the separation between pillared layers increases as the alkylene chain length increases.

A feature of the $n = 10$ material (**3**) is the presence of a P−O−H group from the diphosphonic acid within the structure. The presence of the P−O−H group indicates that it is not a fully condensed structure, unlike all the other pillared members of this series. This feature was

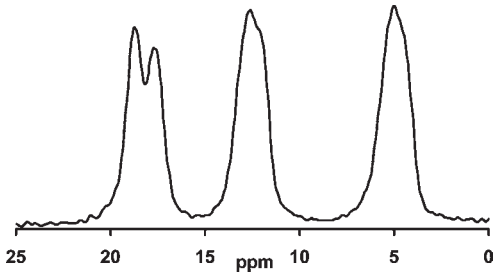

Figure 4. ^{31}P solid-state MAS NMR spectrum of **2**.

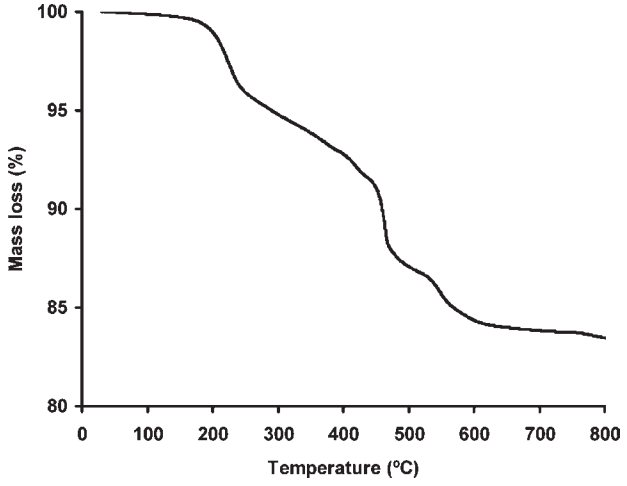

Figure 5. Thermogravimetric analysis trace of **2**.

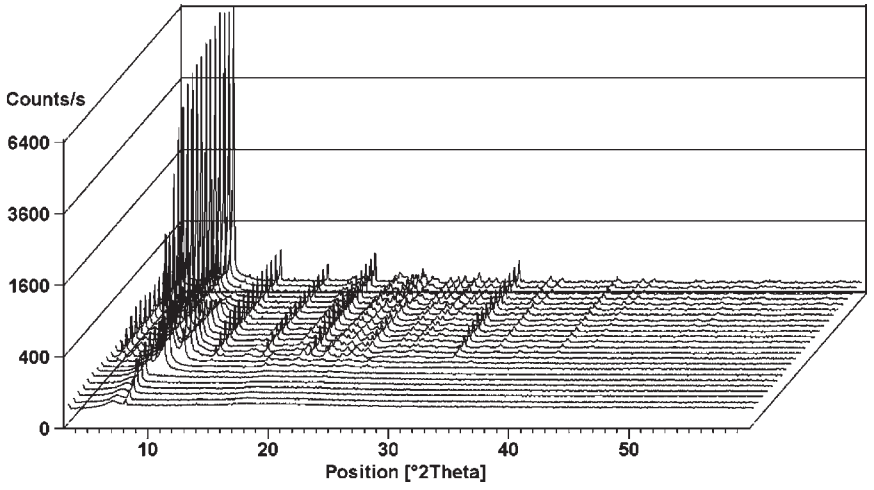

Figure 6. Thermodiffraction patterns of **2**. The temperature at which the patterns were collected, starting from the back of the thermodiffraction stack plot, were 35 °C, 50 °C, and then at intervals of 30 °C up to 710 °C.

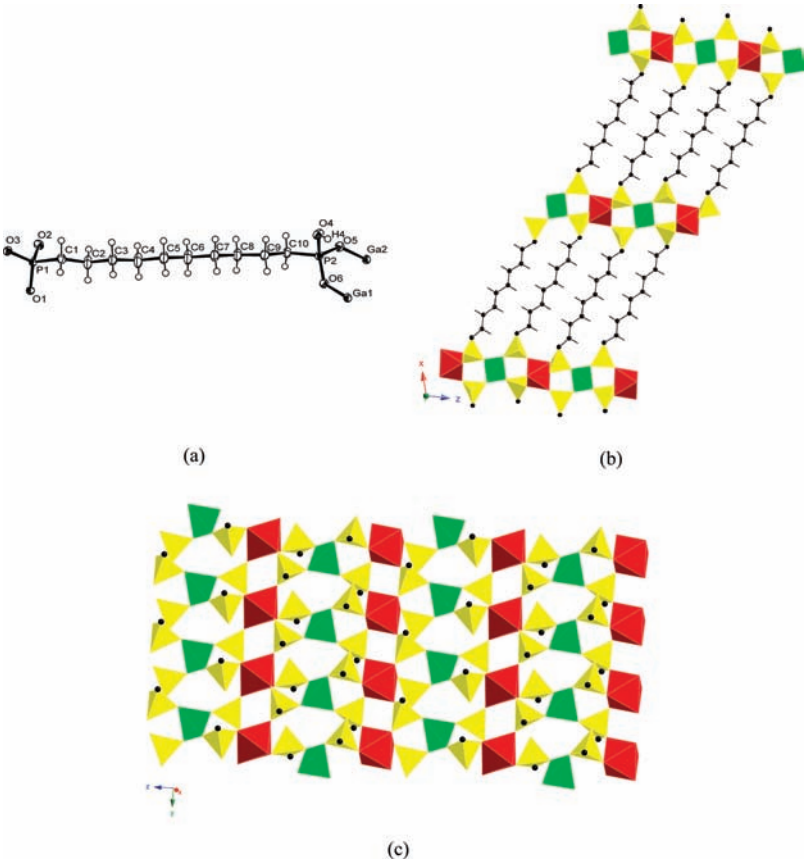

Figure 7. (a) Asymmetric unit of $Ga(HO_3PC_{10}H_{20}PO_3)$ (**3**) with anisotropic atomic displacement ellipsoids shown at the 50% probability level. (b) A polyhedral/ball-and-stick representation of **2** viewed along the *b* axis. (c) A polyhedral/ball-and-stick representation of the Ga−P−O hybrid layer viewed along the *c* axis. Key: octahedral GaO_6 red, tetrahedral GaO_4 light green, tetrahedral PCO_3 yellow, carbon black spheres, hydrogen small gray spheres.

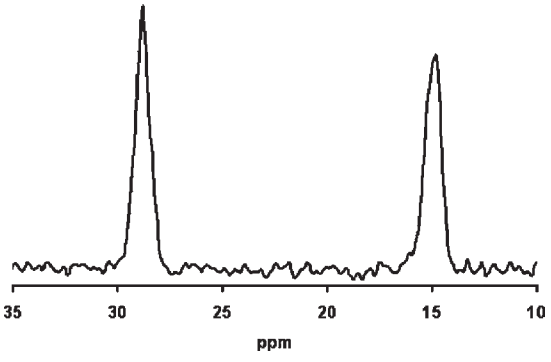

Figure 8. ^{31}P solid-state MAS NMR spectrum of **3**.

observed only in the $n = 10$ member of this pillared series, and notably it is also found only in the longer chain member, $n = 9$, of the only other series of neutral metal diphosphonate materials to be reported,[16] suggesting that full condensation of all the $-PO_3$ group oxygen atoms might become kinetically less favorable as the alkylene chain length increases.

The structural diversity in these gallium alkylenediphosphonates is broadened by the different coordination geometry that the trivalent gallium cations can adopt. Trivalent gallium is known to be coordinated by 4, 5, or 6 species in microporous materials,[23,43] and the gallium alkylenediphosphonate compounds discussed here, with $n = 1$, 2, 3, 5, and 10, contain either tetrahedrally or octahedrally coordinated Ga^{3+} ions. The $n = 3$, 5, and 10 gallium alkylenediphosphonates possess an added dimensionality of structural complexity as they all contain both tetrahedrally and octahedrally coordinated Ga^{3+} ions. This is in contrast to the aluminum alkylenediphosphonate compounds, $n = 2$, 3, and 4, synthesized using this HF/pyridine/water solvent system, in which Al^{3+} ions are always octahedrally coordinated.[24−26] The behavior of gallium in readily forming different coordination polyhedra within a particular neutral metal diphosphonate substructure also contrasts with the tendency of the transition metal cations in series of compounds containing neutral transition metal alkylenediphosphonate substructures formed under similar conditions. In these latter series the transition metal cation tends to adopt only one type of metal coordination polyhedron in any substructure, particularly when the transition metal is present in one oxidation state only within the material.[16,20,21] The use of a post-transition metal cation in the syntheses of these metal alkylenediphosphonate series provides an additional degree of complexity of the formed structures

(40) Burkholder, E.; Golub, V.; O'Connor, C. J.; Zubieta, J. *Inorg. Chem.* **2004**, *43*, 7014.
(41) Bonavia, G.; Haushalter, R. C.; O'Connor, C. J.; Zubieta, J. *Inorg. Chem.* **1996**, *35*, 5603.
(42) Harvey, H. G.; Teat, S. J.; Tang, C. C.; Cranswick, L. M.; Attfield, M. P. *Inorg. Chem.* **2003**, *42*, 2428.
(43) Munch, V.; Taulelle, F.; Loiseau, T.; Ferey, G.; Cheetham, A. K.; Weigel, S.; Stucky, G. D. *Magn. Reson. Chem.* **1999**, *37*, S100.

because of the different metal coordination environments that can coexist in a particular structure.

Conclusions

Solvothermal techniques have been used to prepare a series of gallium diphosphonate materials. Even though all the materials are produced from gels containing the same chemical components under similar conditions, the structural diversity observed is large. In terms of structure design it is apparent that pillared materials are formed when the alkylene chain length is greater than a methylene group, and the separation of layers by these pillars increases in direct relation to the length of the organic linker. Comparison of these gallium alkylenediphosphonates with the extensive family of oxovanadium diphosphonates reveals some comparable trends. The first is that the products of the reactions transform from being 3-dimensional pillared materials to materials containing pillared slabs, and back to 3-dimensional pillared materials as the alkylene chain length increases. Also, as the alkylene chain increases the full condensation of all the P−O bonds of each $-PO_3$ group in the resulting materials appears less likely. The use of a post-transition metal in the formation of this series of metal alkylenediphosphonate materials has also added an additional degree of complexity through the possibility of forming various metal coordination environments within the same compound. The tendency of gallium to exhibit this behavior makes it more difficult to predict the type of structure that will form and to separate aspects of the formed structures influenced by the metal cation or alkylenediphosphonate framework components. It seems that complete structure predictability in this system is not currently possible, except for the general statement that the layer separation increases with alkylene chain length. However, comparative studies with other metal diphosphonate systems allow more general design principles to be developed, such as the influence of tether length on degree of condensation and type of pillared material that is formed, that will aid the formation of more general synthetic protocols to guide the formation of common structural elements and the properties of these solids.

Acknowledgment. The authors thank Dr. D. Apperley of the EPSRC Solid State NMR Service, University of Durham, U.K. for collection of the SS MAS NMR data, the EPSRC National Crystallography Service synchrotron component at Station 9.8, Daresbury Laboratory, and the STFC (formerly CCLRC) for the single-crystal X-ray data for compound **3**, and the Chemical and Materials Analysis Service, Newcastle University, for collection of the microprobe EDX and TGA data. M.P.A. thanks the Royal Society for provision of a University Research Fellowship, and Z.Y. thanks ORS and EPSRC for financial support.

Supporting Information Available: The powder XRD data and CIF files for compounds **1**, **2**, and **3**. This material is available free of charge via the Internet at http://pubs.acs.org.